

Supporting Information

A Fast Species Redistribution Approach to Accelerate Kinetic Monte Carlo Simulation for Heterogeneous Catalysis

Xiao-Ming Cao^{a, *}, Zheng-Jiang Shao^a and P. Hu^{a, b}

^a Key Laboratory for Advanced Materials, Centre for Computational Chemistry and Research Institute of Industrial Catalysis, School of Chemistry and Molecular Engineering, East China University of Science and Technology, 130 Meilong Road, Shanghai, P. R. China 200237

^b School of Chemistry and Chemical Engineering, The Queen's University of Belfast, Belfast BT9 5AG, U.K.

Table of Content_Toc15763615

S1 Universal Lattice KMC Framework	3
S1.1 Generic 2D/3D lattice Representation	3
S1.2 Surface Configuration and Lattice Site Representations	4
S1.3 Elementary Reaction Representation	5
S2 Elementary Reactions Representation for CO Oxidation over Pt(100)	7
S3 Local Configuration Changes for KMC Events	10
S4 Chemical Reaction Kinetics and Parameters	12
S5 Standard KMC Algorithm	15
S6 Standard Lattice KMC Flow Description	15
S7 Lattice KMC Flow Description with Lateral Interactions	18
S8 Comparison to Experimental Results for CO oxidation over Pt(111)	20
S9 Redistribution Interval Test	22

S1 Universal Lattice KMC Framework

S1.1 Generic 2D/3D lattice Representation

One problem for different kMC implementations is the lacking of a universal way for building detailed or complex lattice grid with various possible adsorption sites. In our kMC simulation, we construct the kMC lattice model for 2D lattice surface within a three-dimensional lattice space using a generic representation method, taking the types of adsorption sites into consideration.

In the generic representation method, each lattice site \bar{s}_i can be presented by a four-dimension vector:

$$\bar{s}_i = [x_i \ y_i \ z_i \ b_i]^T, \bar{s}_i \in C(\bar{L}) \quad \backslash * \text{MERGEFORMAT} \quad (1)$$

where the first three entries are the direct coordinates for origin site of a unit cell in 3-dimensional vector space, and the last entry is the order number of extended site in a cell. \bar{L} is a $4 \times N_L$ lattice matrix which consists of all the sites as column vectors, and C denotes the 4-D column space of the lattice matrix in which all the lattice sites are included and N_L is the site number in lattice.

The whole lattice grid for the kMC simulation is constructed by expanding the unit cell periodically. In the unit cell, we can define any number of extra sites besides the origin site (site 0) which is essential for lattice construction. All sites defined in the unit cell will be called “basis site” in the rest of the paper. Then, the fractional coordinate for site i , \bar{c}_i can be calculated using

$$\bar{c}_i = [x_i y_i z_i]^T + \bar{c}_{b_i} \quad \backslash * \text{MERGEFORMAT} \quad (2)$$

, where \bar{c}_{b_i} denotes the coordinate of basis site i with respect to the origin site of unit cell and $[x_i y_i z_i]^T$ refers to the fractional coordinate of origin site in unit cell.

The periodic 3-dimensional lattice grid then can be presented in a $4 \times (N_x \times N_y \times N_z \times N_b)$ matrix. N_x , N_y and N_z are respectively the repeat numbers of unit

cell along axis x , y and z . Eq. * MERGEFORMAT (3) shows a matrix presentation example of 3-dimensional lattice grid \bar{L} with 3 extra basis sites ($N_b=3$) in each unit cell, some of which can be used as extra adsorption sites in practice and N_L is the total site number in the whole grid.

$$\bar{L} \equiv \begin{bmatrix} x_0 & x_0 & x_0 & \cdots & x_{N_L-2} & x_{N_L-1} \\ y_0 & y_0 & y_0 & \cdots & y_{N_L-2} & y_{N_L-1} \\ z_0 & z_0 & z_0 & \cdots & z_{N_L-2} & z_{N_L-1} \\ b_0 & b_1 & b_2 & \cdots & b_1 & b_2 \end{bmatrix} \quad \backslash * \text{ MERGEFORMAT (3)}$$

Benefitting from the generic lattice representation method, we can easily extend the method to map the periodic surface structure into the lattice grid with arbitrary complexity.

S1.2 Surface Configuration and Lattice Site Representations

After building the lattice mesh, the grid can be treated as a skeleton and will be filled with multiple layers containing information about the element types, site types and the relative location of its n th nearest neighbors to construct the specific surface configuration and lattice site.

Each site at lattice can be bound with a specific species and site type to represent adsorbate type and lattice site type respectively. Thus, the layer can be represented by a vector \bar{C} with length N_L ,

$$\bar{C} \equiv \left[t_{[x_0 y_0 z_0 b_0]}, t_{[x_0 y_0 z_0 b_1]}, \cdots, t_{[x_i y_i z_i b_i]}, \cdots, t_{[x_{N_x-1} y_{N_y-1} z_{N_z-1} b_{N_b-1}]} \right]^T \quad \backslash *$$

MERGEFORMAT (4)

where the $t_{[x_i y_i z_i b_i]}$ denotes a species or site type mapping on a grid node and its coordinate is $[x_i y_i z_i b_i]$. The type binding to a lattice node could be any one of N_s possible types set:

$$t_{[x_i y_i z_i b_i]} \in \{0, 1, 2, \cdots\}^{N_s} \quad \backslash * \text{ MERGEFORMAT (5)}$$

. Each entry in the set has a point-to-point mapping to the actual type species such as

CO, O, vacant lattice site and so on.

For the lattice with more than one site type like metallic oxide catalysts, the site type is a vital descriptor that can help us to reduce the complexity of the lattice sites abstraction or surface coarse graining process. With specified site types, we can easily involve the information about site changes as a part of kMC elementary steps. The surface reconstruction thus can also be simulated in kMC implementation similarly with the elementary reaction representation methods described in the next part.

S1.3 Elementary Reaction Representation

The overall kMC simulation is a process where the system jumps from one state to another state, namely, from an energy basin to another energy basin on potential energy surface, generating a Markov chain or a configuration trajectory. The connection between any two states is an elementary reaction which can invoke the change of system state. Here we demonstrate the generic representation methods for the elementary reactions in our on-lattice kMC simulation.

On the lattice grid \bar{L} with initialized configuration \bar{C} and site types \bar{S} , all M possible elementary reactions \bar{R} can be formulated as

$$\bar{R} \equiv [P_0, P_1, \dots, P_M]^T \quad \backslash * \text{MERGEFORMAT (6)}$$

where P_i denotes one of elementary process and contains four main components:

- (i) Initial local configuration \bar{C}_i and local site types \bar{S}_i with m elements,

$$\bar{C}_i \equiv [t_0, t_1, \dots, t_{m-1}]^T \quad \backslash * \text{MERGEFORMAT (7)}$$

$$\bar{S}_i \equiv [st_0, st_1, \dots, st_{m-1}]^T \quad \backslash * \text{MERGEFORMAT (8)}$$

- (ii) Final local configuration \bar{C}'_i and local site types \bar{S}'_i with same m elements,

$$\bar{C}'_i \equiv [t'_0, t'_1, \dots, t'_{m-1}]^T \quad \backslash * \text{MERGEFORMAT (9)}$$

$$\bar{S}'_i \equiv [st'_0, st'_1, \dots, st'_{m-1}]^T \quad \backslash * \text{MERGEFORMAT (10)}$$

- (iii) Relative positions for all m local sites c_j with respect to the local center (the first elements in local environment),

$$\overline{Coord}_i \equiv [c_0, c_1, \dots, c_{m-1}]^T \quad \backslash * \text{MERGEFORMAT (11)}$$

- (iv) Reaction rate k_i for process i calculated using rate theory equations (see **Section S4**).

More graph representation examples of elementary reactions in CO oxidation over a Pt(100) surface are listed in **Section S2**. In order to describe the reaction kinetic behavior on lattice more realistically, the details about orientation and adsorption sites of multidentate species can also be specified. In our kMC implementation, we take all information about multidentate adsorbates and orientation into account by treating atoms in a molecule as directed nodes including extra direction information. **Fig. S2** shows an example of elementary process for O₂ molecular adsorption on two adjacent bridge sites.

S2 Elementary Reactions Representation for CO Oxidation over Pt(100)

Each elementary reaction in kMC simulation can be firstly abstracted to two connected graphs and then represented by two linear tables which contains all necessary entries for pattern matching. The abstraction for a CO gas molecule adsorption process is displayed in **Fig. S1**: a CO adsorbed on the bridge site of Pt (100) surface with its nearest neighbors vacant. Furthermore, as the next step, the dissociation of O₂ molecule can be easily represented similarly (see **Fig. S3**). The diffusion process is the key in this work and it can be easily represented in the same way (see **Fig. S4**).

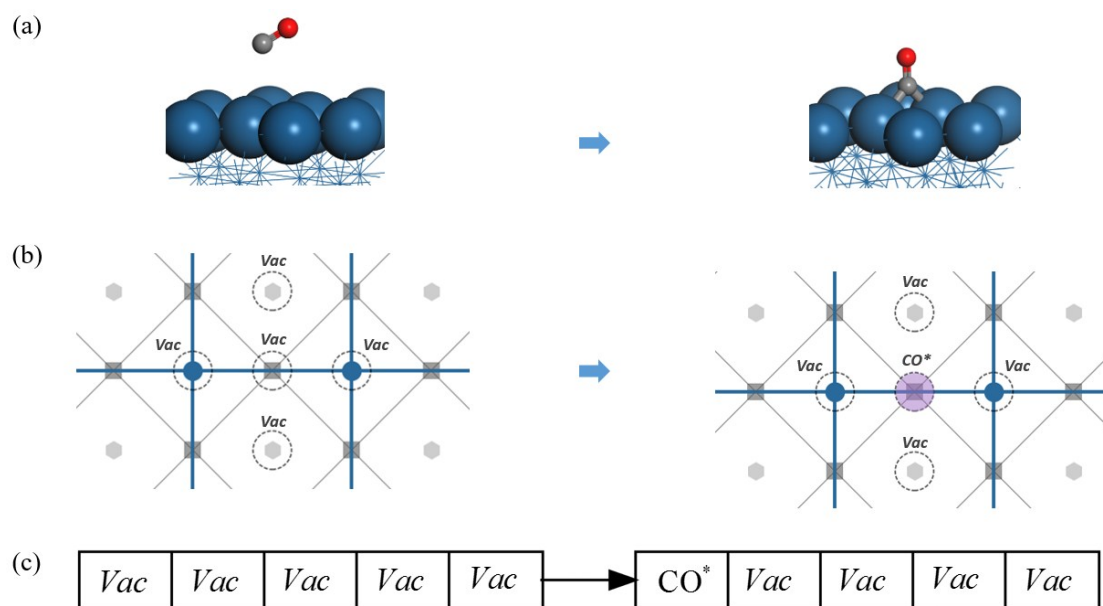


Fig. S1. The abstraction process for the CO adsorption. (a) The side view the CO adsorption process. (b) The local configurations before (left panel) and after (right panel) a CO molecule adsorbing on a bridge site. (c) The linear table containing the species types before and after adsorption process occurring used for configuration pattern matching.

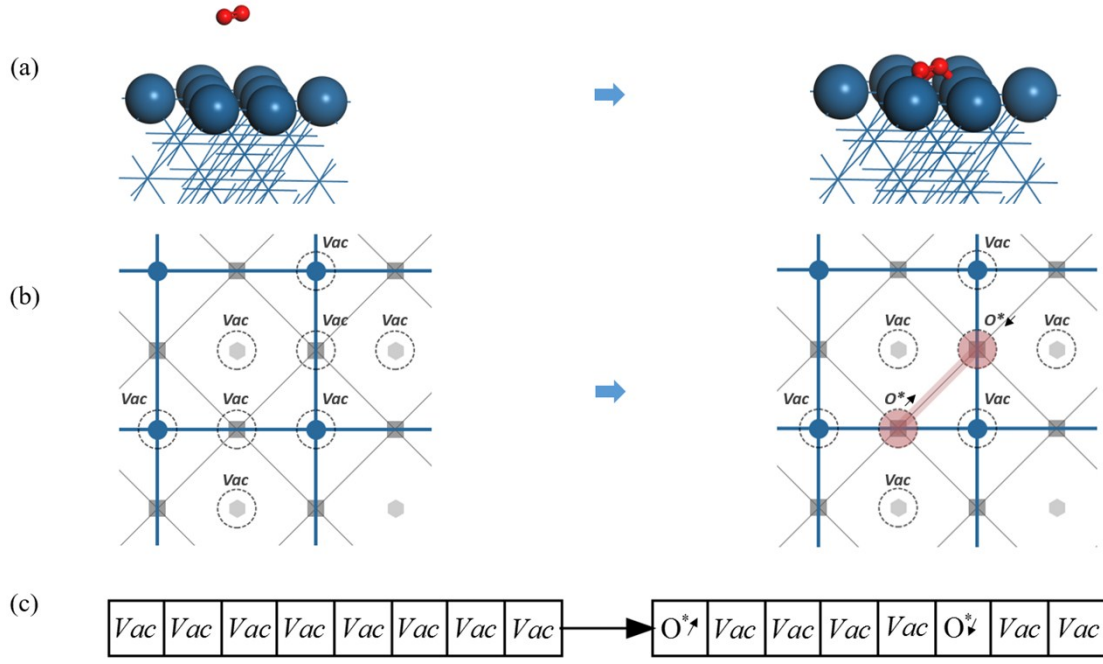


Fig. S2. The description of O_2 molecule adsorbing to 2 bridge sites on Pt (100) surface under the exclusion rule defined above. (a) The three-dimensional side view of O_2 molecular adsorption process (from the left panel to right). (b) The graph representation of the local configuration change invoked by the molecular adsorption process. O_2 molecule is plotted in a graph with two directed nodes connected by an edge (red). (c) The initial and final pattern match lists for that process with all species types sorted by their positions relative to the center species (red circle pointing to the upper right direction).

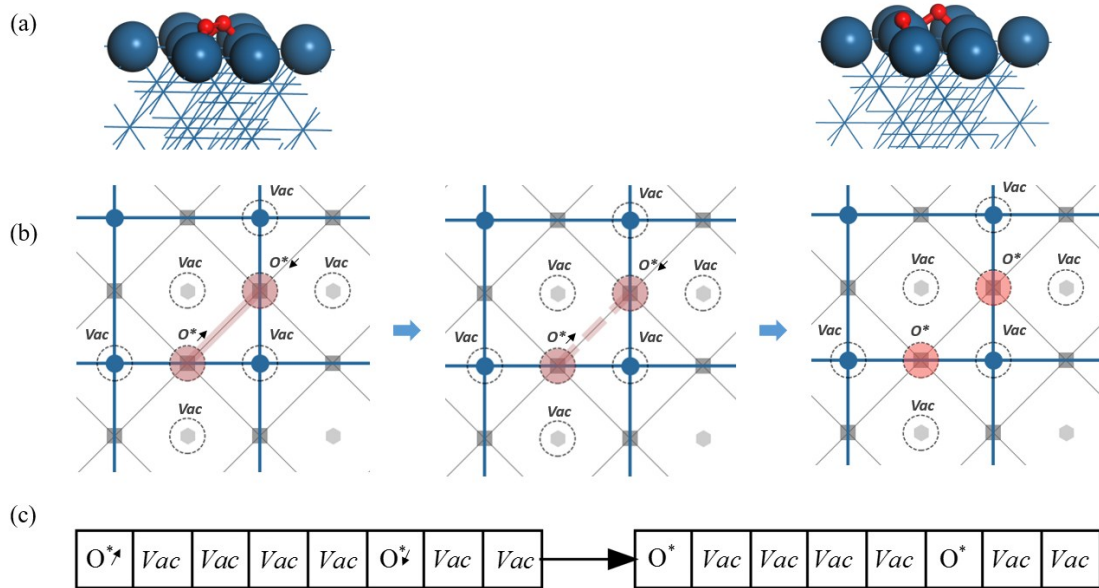


Fig. S3. The corresponding side view (a), graph representation (b) and species match lists (c) for the O_2

dissociation reaction on Pt (100) surface.

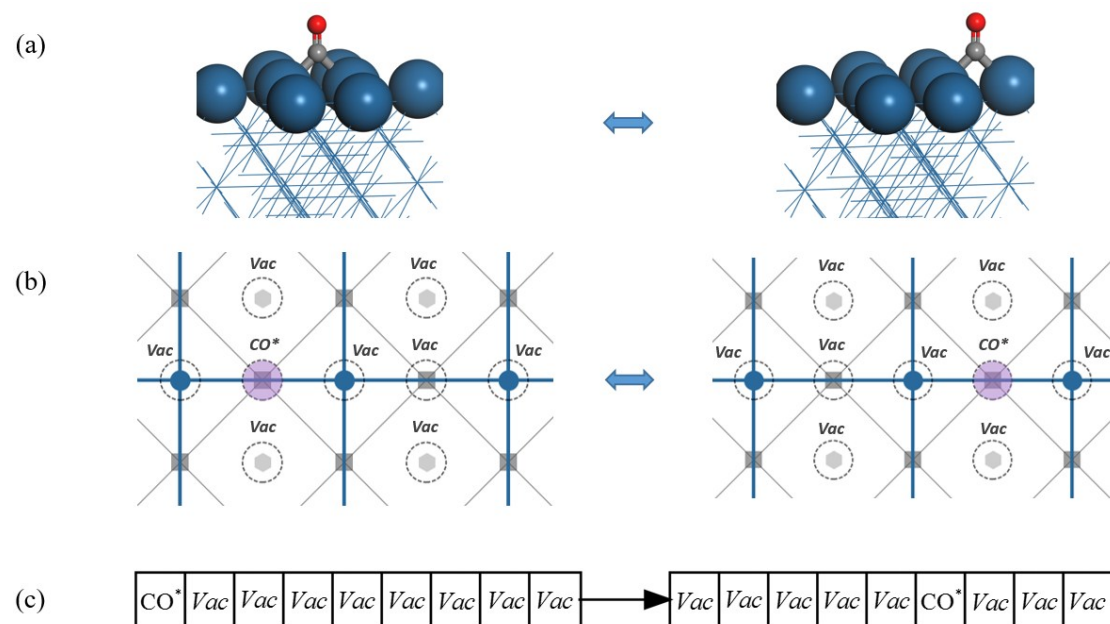


Fig. S4. The side view (a), graph representation (b) and species match lists (c) for the CO symmetry diffusion process on Pt (100) surface.

S3 Local Configuration Changes for KMC Events

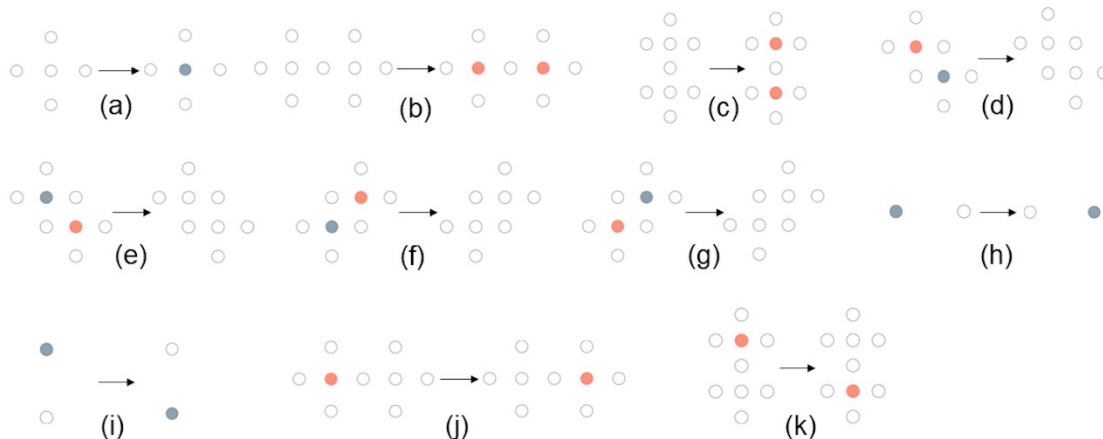


Fig. S5. Local configuration (environment) changes for kMC events of CO oxidation elementary reactions over Pt(100) surface: CO adsorption: (a); O₂ dissociative adsorption: (b) and (c); CO* and O* coupling: (d), (e), (f) and (g); CO* diffusion: (h) and (i); O* diffusion: (j) and (k). The grey circle represents CO* and red circle is O*.

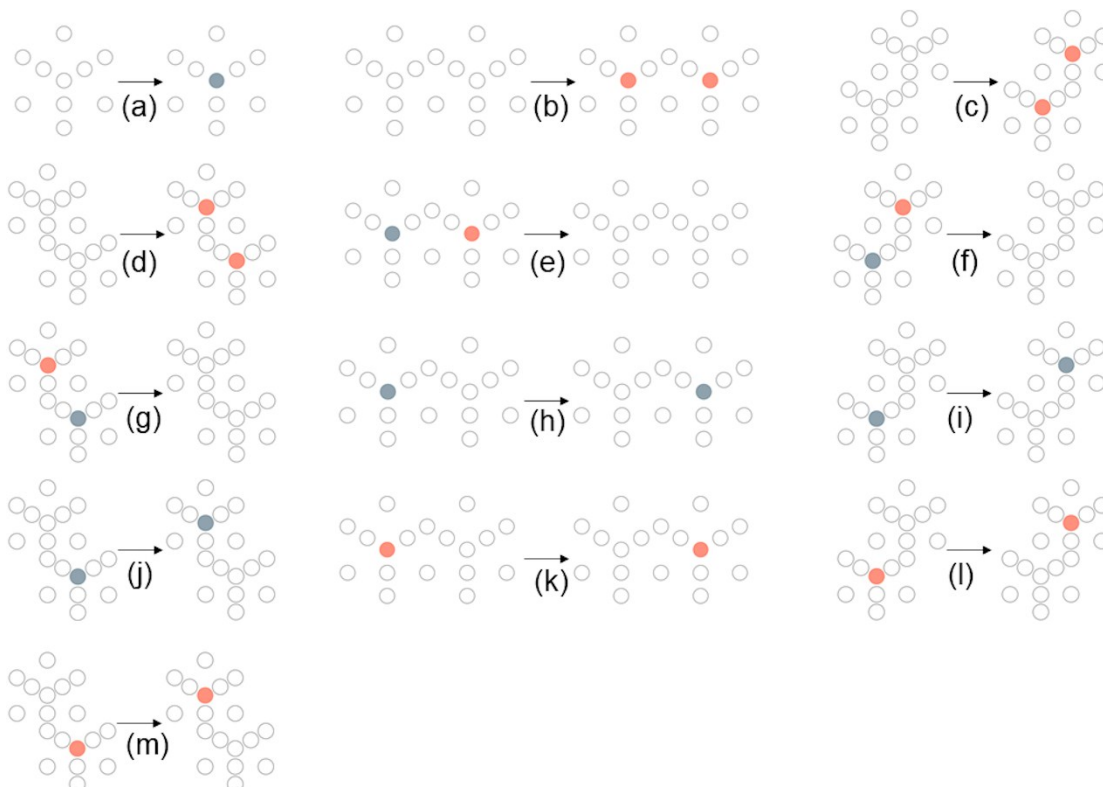


Fig. S6. Local configuration (environment) changes for kMC events of CO oxidation elementary reactions over Pt(111) surface: CO adsorption: (a); O₂ dissociative adsorption: (b), (c) and (d); CO* and O* coupling: (e), (f) and (g); CO* diffusion: (h), (i) and (j); O* diffusion: (k), (l) and (m).

and O* coupling: (e), (f) and (g); CO* diffusion: (h), (i) and (j); O* diffusion: (k), (l) and (m). The grey circle represents CO* and red circle is O*.

S4 Chemical Reaction Kinetics and Parameters

In our work, we used collision theory to handle the kinetics of molecule adsorption process and the equivalent adsorption barrier (G_a) for transition state could be derived¹⁻².

The adsorption/desorption process rates could be described by the ideal gas laws by measuring the collision rate of particles with mass m_i impinging onto a surface unit cell with an area of A_{uc} at temperature T and pressure p_i according to the collision theory, according to the collision theory and transition state theory, the reaction rate on per site could be written as:

$$r^{ads}(T) = S_i(T) \frac{p_i A_{uc}}{\sqrt{2\pi m_i k_B T}} = \frac{k_B T}{h} \exp\left(-\frac{G_a^{ads}}{k_B T}\right) \frac{P_i}{P_0} = k^{ads} \frac{P_i}{P_0} \quad (12)$$

where S_i is the local sticking coefficient governing the sticking probability of the

impinging particles to the free sites of surface, k_B is the Boltzmann constant, p_0 is the standard gas pressure and k^{ads} is the adsorption rate constant. Hence we could get an equation about adsorption barrier:

$$G_a^{ads} = -k_B T \ln\left(\frac{p_0 A_{uc} h}{k_B T \sqrt{2\pi m_i k_B T}}\right) \quad (13)$$

Accordingly, for the desorption process, the corresponding desorption rate constant k^{des} is calculated according to the equilibrium constant K and adsorption rate constant k^{ads} :

$$k^{des} = \frac{k^{ads}}{K} \quad (14)$$

Reaction and diffusion processes of adsorbed intermediates on the lattice can be treated directly within transition state theory framework. The rate for an elementary reaction can be given by

$$r^{react} = \frac{k_B T}{h} \exp\left(-\frac{G_a^{react}}{k_B T}\right) \quad \backslash * \text{MERGEFORMAT} \quad (15)$$

Similarly, the rate for an adsorbed particle hopping from one site to another can be written as

$$r^{diff} = \frac{k_B T}{h} \exp\left(-\frac{G_a^{diff}}{k_B T}\right) \quad \backslash * \text{MERGEFORMAT} \quad (16)$$

where G_a^{react} and G_a^{diff} are free barriers of reaction and diffusion processes.

The sticking coefficients used in our kinetic simulations are all from measured data in experimental references³⁻⁶ (see **Table S1**). The energy of adsorbates are corrected using zero point energy (ZPE), internal energy (U) and entropy (TS)⁷. The energetic corrections for elementary reactions on Pt(111) and Pt(100) in kinetic modeling (T=500K) including zero point energy (ZPE), internal energy (U) and entropy (TS) are listed in **Table S2** and **Table S3**.

Table S1 Sticking coefficients of CO and O₂ on Pt(111) and Pt(100) used in kinetic simulations.

Surface	S(CO)	S(O ₂)
Pt(111)	0.89	0.08
Pt(100)	0.6	0.1

Table S2. Energy corrections (zero point energy, internal energy, entropy) for elementary reactions in CO oxidation over Pt(100) surface (T = 500K).

Reaction	Barrier Correction/eV			Reaction Energy Correction/eV		
	ΔZPE	ΔU	$T\Delta S$	ΔZPE	ΔU	$T\Delta S$
$\text{CO}_{(g)} + *_{(b)} \leftrightarrow \text{CO}^*_{(b)}$	/	/	/	0.07	0.05	-0.73
$\text{O}_{2(g)} + 2*_{(b)} \rightarrow 2\text{O}^*_{(b)}$	/	/	/	0.04	0.05	-0.79
$\text{CO}^*_{(b)} + \text{O}^*_{(b)} \leftrightarrow \text{CO}_{2(g)}$	-0.01	-0.03	-0.04	0.03	-0.09	0.68

Table S3. Energy corrections (zero point energy, internal energy, entropy) for elementary reactions in CO oxidation over Pt(111) surface (T = 500K).

Reaction	Barrier Correction/eV			Reaction Energy Correction/eV		
	ΔZPE	ΔU	$T\Delta S$	ΔZPE	ΔU	$T\Delta S$
$\text{CO}_{(g)} + *_{(b)} \leftrightarrow \text{CO}^*_{(b)}$	/	/	/	0.05	0.06	-0.74
$\text{O}_{2(g)} + 2*_{(b)} \rightarrow 2\text{O}^*_{(b)}$	0.05	0.07	-0.88	0.04	0.06	-0.83
$\text{CO}^*_{(b)} + \text{O}^*_{(b)} \leftrightarrow \text{CO}_{2(g)}$	-0.001	-0.03	-0.03	0.05	-0.1	0.71

S5 Standard KMC Algorithm

The evolution of the system over time in the stochastic model is described by the chemical master equation (CME) which is derived from first principles⁸⁻⁹.

$$\frac{dP(c,s,t)}{dt} = \sum_{c',s' \neq c,s} \left[P(c',s',t) k_{c',s' \rightarrow c,s} - P(c,s,t) k_{c,s \rightarrow c',s'} \right] \quad \backslash *$$

MERGEFORMAT (17)

In this equation, $P(c,s,t)$ denotes the probability to find the system in configuration c with lattice site types s at time t ; $k_{c,s \rightarrow c',s'}$ is the transition probability of the reaction that transfer the system state from (c,s) to (c',s') . The exponential distribution function $p(t)$, which determines the time until the reaction takes place, can be derived¹⁰⁻¹¹,

$$P(t) = k_{tot} \exp(-k_{tot}t) \quad \backslash * \text{ MERGEFORMAT (18)}$$

with the expected value (the average transition time τ)

$$\tau = \int_0^{\infty} t p(t) dt = \frac{1}{k_{tot}}, \quad \backslash * \text{ MERGEFORMAT (19)}$$

where k_{tot} is the total escape or transition rate from the current system state.

Then we can get an exponentially distributed random number t_{draw} drawn from the distribution in Eq. * MERGEFORMAT (18) with a uniform random number r sampled in the range (0, 1), which is generated with Mersenne twister pseudo-random number generating algorithm¹² in our implementation,

$$t_{draw} = - \left(\frac{1}{k_{tot}} \right) \ln(r) \quad \backslash * \text{ MERGEFORMAT (20)}$$

S6 Standard Lattice KMC Flow Description

0. Simulation starts.

1. Lattice grid abstraction: define unit cell with extra possible adsorption sites and

expand it to an abstract lattice grid \overline{L} where all processes in kMC simulation can occur.

2. Configuration initialization: fill all lattice sites constructed in step 1 with possible species including molecular orientation and multidentate species information. The default configuration is an empty surface, namely, all the sites occupied by “vacant” species.
3. Site types initialization: initialize all site types in a similar way with configuration initialization.
4. Reaction kinetics calculation: (i) parse reaction equation expressions and energy data; (ii) calculate reaction rates for all elementary reaction; (iii) initialize all corresponding elementary processes for kMC simulation.
5. Initial pattern matching: traverse the entire lattice site and match the local configuration and site types with all processes for each site to construct a process table containing information about site availability. With the help of the table, we can easily obtain the total rate k_{tot} for all n available processes.

$$k_{tot} = \sum_{i=1}^n k_i N_{avail}^i \quad \backslash * \text{MERGEFORMAT (21)}$$

where k_i is the transition rate for reaction i , N_{avail}^i is the number of sites where reaction i can occur.

Further, the incremental probability table \overline{P} can also be constructed for process picking in each single kMC step,

$$\overline{P} = \frac{\left[\sum_{i=1}^l k_i N_p \sum_{i=1}^2 k_i N_p \cdots \sum_{i=1}^n k_i N_i \right]^T}{k_{tot}} \quad \backslash * \text{MERGEFORMAT (22)}$$

6. Reaction pathway picking: (i) generate a uniform distributed random number r_1 in range (0, 1]; (ii) select the reaction to be performed by comparing r_1 to entries in \overline{P} using a binary search with complexity $O(\log(n))$.
7. Reaction site picking: draw an available site from the available sites for reaction

picked in step 6 randomly.

8. System evolution: perform the process picked in step 6 on the site chosen in step 7 by updating the configuration and site types according to the process definition.
9. Local environment re-matching: (i) collect sites affected by the performed reaction on the lattice, (ii) match all processes on these local affected sites and update related information such as processes table, configuration and site types pattern match lists and so on.
10. Time propagation: draw a random number r_2 between 0 and 1, and the simulation time is propagated by

$$\Delta t = \frac{-\ln(r_2)}{k_{tot}} \quad \backslash * \text{MERGEFORMAT (23)}$$

11. Repeat from step 6 until the maximum allowed simulation time or step number is reached.
12. Data post-processing: after the kMC iteration is over, all related data collected on-the-fly (coverages, simulation time, reaction frequency ...) will be written to local files which could be used for data post-processing.
13. Termination.

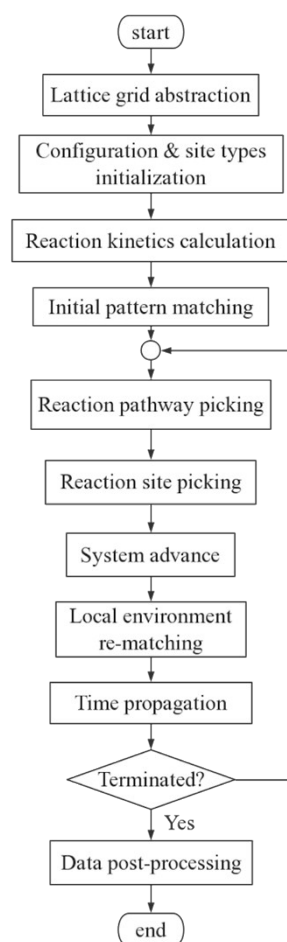


Fig. S7. Flowchart of the standard lattice kMC algorithm.

S7 Lattice KMC Flow Description with Lateral Interactions

0. Simulation starts.
1. Lattice grid abstraction: define unit cell with extra possible adsorption sites and expand it to an abstract lattice grid \overline{L} where all processes in kMC simulation can occur.
2. Configuration initialization: fill all lattice sites constructed in step 1 with possible species including molecular orientation and multidentate species information. The default configuration is an empty surface, namely, all the sites occupied by “vacant” species.
3. Site types initialization: initialize all site types in a similar way with configuration initialization.
4. Initial pattern matching (process matching): traverse all lattice sites and match each site with possible elementary process to construct a table of the availability and total rate of each process. Different from the standard kMC flow, with interactions considered at each site where a process is possible to occur, the rate is calculated on-the-fly. Then the total rate R_i of a process i does not equal to fixed rate multiplying available site number ($k_i N_{avail}^i$) anymore. It is now obtained by summing the updated local rate for each site where the process is available.

$$R_i = \sum_{j=1}^{N_i} r_j \quad \backslash * \text{MERGEFORMAT} \quad (24)$$

where N_i is the available sites for process i , and r_j is the locally updated rate at site j .

5. Process incremental probability table creation: similar with standard kMC, the incremental rate table \overline{P} for processes can be established for process picking,

$$\overline{P} = \frac{\left[\sum_{i=1}^l R_1, \sum_{i=1}^2 R_2, \dots, \sum_{i=1}^n R_n \right]^T}{\sum_{i=1}^n R_i} \quad \backslash * \text{MERGEFORMAT} \quad (25)$$

6. Site incremental probability table creation: for a picking process, the site where the process will be performed is chosen using a similar vector \bar{S} of incremental rates:

$$\bar{S} = \frac{[\sum_{i=1}^1 r_1, \sum_{i=1}^2 r_2, \dots, \sum_{i=1}^n r_n]^T}{\sum_{i=1}^n r_i} \quad \backslash * \text{MERGEFORMAT (26)}$$

where r_i is the rate of the process on site i .

7. Reaction process picking: (i) generate a uniform distributed random number r_1 in range (0, 1]; (ii) select the reaction to be performed by comparing r_1 to entries in \bar{P} using a binary search with complexity $O(\log(n))$.
8. Reaction site picking: different with complete random picking in standard kMC flow, since the rate now may vary over sites even for the same process, we need to draw the site according to the rate related distribution. (i) generate a uniform distributed random number r_2 in range (0, 1]; (ii) select the site by comparing r_2 to entries in \bar{S} using binary search.
9. The remaining of the algorithm flow is identical with the procedure of standard kMC described in **Section S6** above (system evolution, local environment re-matching, time propagation and data post-processing) .

S8 Comparison to Experimental Results for CO oxidation over Pt(111)

We compared our FSR-kMC simulation results with the reported Temperature Programmed-Fluorescence Yield Near Edge Spectroscopy (TP-FYNES) of CO temperature-programmed desorption in the presence of 0.002 Torr O_2 with CO oxidation over the Pt(111) surface¹³. First, we used FSR-kMC to simulate the adsorption process of CO on clean Pt(111) surface ($P(CO) = 2e-7$ Torr, $T=300$ K) and the saturated CO coverage obtained was 0.62ML ($\sim 9.0 \times 10^{14}$ molecules/cm²) which is similar with the experimental data (9.8×10^{14} molecules/cm²). As displayed in **Fig. S9**, we can see that FSR-kMC can also produce the consistent CO coverage trend and temperature range of CO desorption with TP-FYNES experiments: the oxidation begins at around 300 K and is completed at about 330 K.

In addition to the temperature-programmed spectrum simulation, we also estimated the apparent activation energy of CO oxidation using FSR-kMC simulation. As displayed in **Fig. S10**, the simulated apparent activation energy for CO oxidation below 6.7×10^{14} molecules/cm² coverage of CO with 0.02 Torr of O_2 is 13.31 kcal/mol, which is close to the experimental measurement (12.3 kcal/mol)¹³.

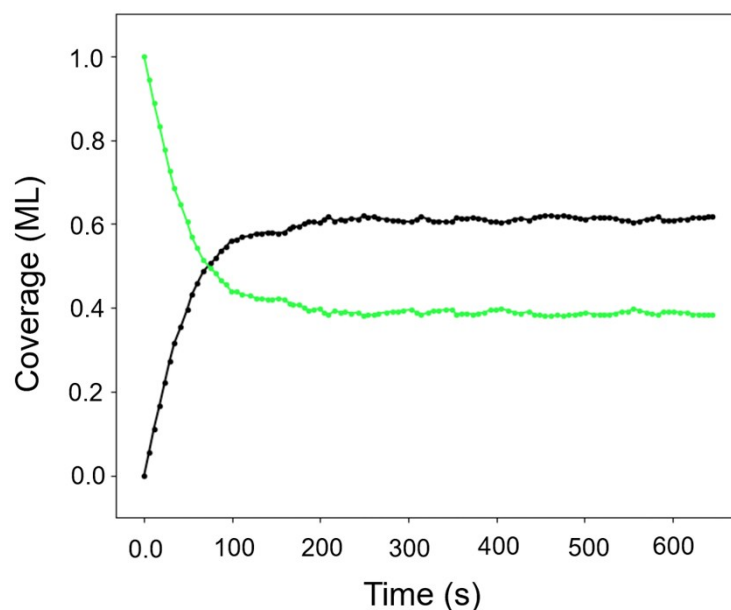


Fig. S8. The surface adsorbate coverage evolution trajectories versus time simulated for CO adsorption

process using FSR kMC. The coverage trajectories of CO* and vacant site are plotted with black and green lines respectively.

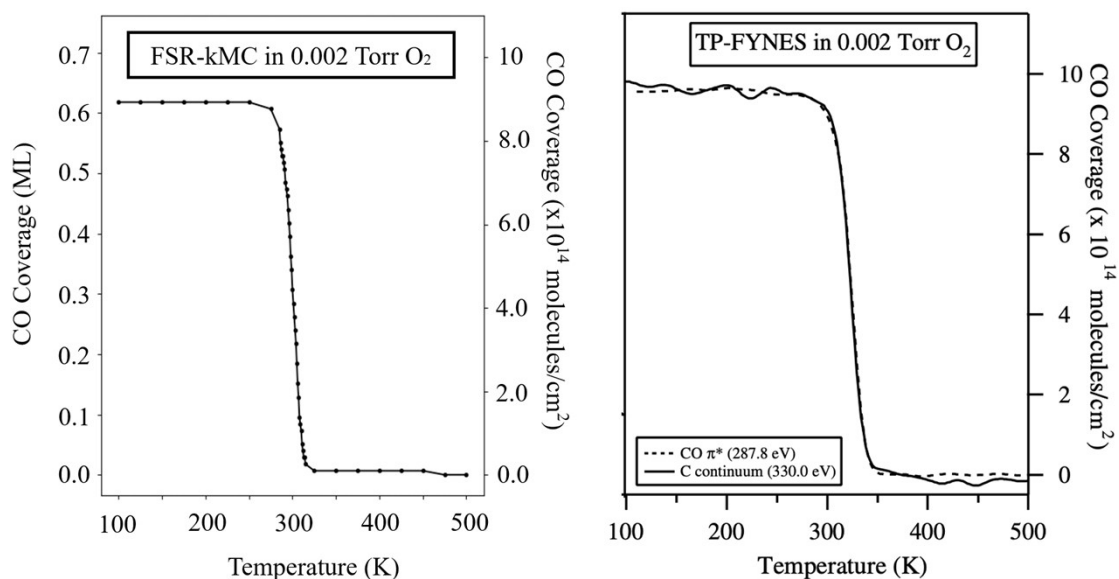


Fig. S9. FSR-kMC simulation (left panel) and TP-FYNES (right panel) of a saturated CO coverage heated in 0.002 Torr of flowing oxygen.

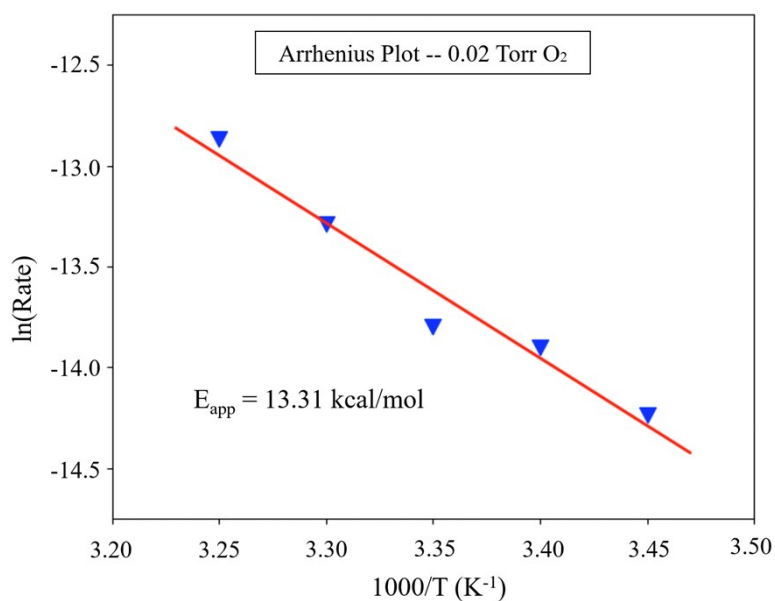


Fig. S10. Arrhenius plot simulated using FSR-kMC method showing apparent activation energy for CO oxidation below 6.7×10^{14} molecules/cm² coverage of CO in 0.02 Torr flowing O₂.

S9 Redistribution Interval Test

We tested the influence of the times interval for the redistribution process utilizing the case of CO oxidation over Pt(100) under the same UHV condition in **Section 4.1**. **Table S4** displays the calculated TOF values with different redistribution intervals.

Table S4. Simulated steady state TOFs using different redistribution interval for CO oxidation over Pt(100) case.

Redistribution Interval	TOF (s ⁻¹)
1	1.24
100	1.23
200	1.23
300	1.24
400	1.23
500	1.24
600	1.23
700	1.23
800	1.23
900	1.24

References

1. Yuan, H.; Chen, J.; Guo, Y.; Wang, H.; Hu, P., Insight into the Superior Catalytic Activity of MnO₂ for Low-Content NO Oxidation at Room Temperature. *J. Phys. Chem. C* **2018**, *122*, 25365-25373.
2. Tang, Q.-L.; Hong, Q.-J.; Liu, Z.-P., CO₂ Fixation into Methanol at Cu/ZrO₂ Interface from First Principles Kinetic Monte Carlo. *J. Catal.* **2009**, *263*, 114-122.
3. Campbell, C.; Ertl, G.; Kuipers, H.; Segner, J., A Molecular Beam Investigation of the Interactions of Co with a Pt (111) Surface. *Surf Sci.* **1981**, *107*, 207-219.
4. Luntz, A.; Williams, M.; Bethune, D., The Sticking of O₂ on a Pt (111) Surface. *J. Chem. Phys.* **1988**, *89*, 4381-4395.
5. Brodén, G.; Pirug, G.; Bonzel, H., Chemisorption of Co on the Unreconstructed Pt (100) Surface. *Surf Sci.* **1978**, *72*, 45-52.
6. Norton, P.; Griffiths, K.; Bindner, P., Interaction of O₂ with Pt (100): II. Kinetics and Energetics. *Surf Sci.* **1984**, *138*, 125-147.
7. Cao, X.-M.; Burch, R.; Hardacre, C.; Hu, P., Reaction Mechanisms of Crotonaldehyde Hydrogenation on Pt (111): Density Functional Theory and Microkinetic Modeling. *J. Phys. Chem. C* **2011**, *115*, 19819-19827.
8. Quack, M., Ng Van Kampen: Stochastic Processes in Physics and Chemistry. North Holland Publishing Company, Amsterdam 1981. 419 Seiten, Preis: \$76.50. *Ber. Bunsenges. Phys. Chem.* **1983**, *87*, 370-370.
9. Jansen, A., Monte Carlo Simulations of Chemical Reactions on a Surface with Time-Dependent Reaction-Rate Constants. *Comput. Phys. Commun.* **1995**, *86*, 1-12.
10. Lukkien, J.; Segers, J.; Hilbers, P.; Gelten, R.; Jansen, A., Efficient Monte Carlo Methods for the Simulation of Catalytic Surface Reactions. *Phys. Rev. E* **1998**, *58*, 2598.
11. Sickafus, K. E.; Kotomin, E. A.; Uberuaga, B. P., *Radiation Effects in Solids*; Springer Science & Business Media, 2007; Vol. 235.
12. Matsumoto, M.; Nishimura, T., Mersenne Twister: A 623-Dimensionally Equidistributed Uniform Pseudo-Random Number Generator. *ACM Transactions on Modeling and Computer Simulation (TOMACS)* **1998**, *8*, 3-30.
13. Burnett, D. J.; Capitano, A. T.; Gabelnick, A. M.; Marsh, A. L.; Fischer, D. A.; Gland, J. L., In-Situ Soft X-Ray Studies of Co Oxidation on the Pt (1 1 1) Surface. *Surf Sci.* **2004**, *564*, 29-37.